

## Gallium(3+) Binding to Ovotransferrin and Its Half-Molecules: A Multinuclear NMR Study

James M. Aramini, Deane D. McIntyre, and Hans J. Vogel\*

Contribution from the Department of Biological Sciences, University of Calgary, Calgary, Alberta, Canada T2N 1N4

Received June 28, 1994<sup>⊗</sup>

**Abstract:** We have used  $^{13}\text{C}$ ,  $^{69}\text{Ga}$ , and  $^{71}\text{Ga}$  NMR spectroscopy to probe the binding of  $\text{Ga}^{3+}$  to ovotransferrin in the presence of  $^{13}\text{C}$ -enriched carbonate and oxalate. When carbonate is the synergistic anion, two  $^{13}\text{C}$  and  $^{71}\text{Ga}$  signals appear sequentially, corresponding to  $^{13}\text{CO}_3^{2-}$  and  $\text{Ga}^{3+}$  bound to the two metal ion binding sites of the protein. In combination with  $^{13}\text{C}$  NMR studies of the proteolytic half-molecules of ovotransferrin, we found that the metal ion interacts preferentially with the N-site of the intact protein. In the case of oxalate, one observes two pairs of doublets due to the nonequivalent carbonyl carbons of the bound anion in both sites and, again, two overlapping  $^{71}\text{Ga}$  signals. Ovotransferrin exhibits no site preference for  $\text{Ga}^{3+}$  in the presence of oxalate. The  $^{13}\text{C}$  and  $^{71}\text{Ga}$  signals characteristic of this adduct were again assigned using the N- and C-terminal half-molecules of the protein, and we found substantially broader  $^{71}\text{Ga}$  signals for the isolated lobes compared to the intact protein. By exploiting the fact that the bound  $^{71}\text{Ga}$  signals are due to the central ( $m = 1/2 \rightarrow -1/2$ ) transition of this quadrupolar ( $I = 3/2$ ) nucleus and using the observed chemical shifts and line widths of the protein-bound  $^{71}\text{Ga}$  signals at two magnetic fields ( $B_0 = 9.4$  and  $11.7$  T), we have calculated values for the quadrupole coupling constant ( $\chi$ ) of the  $^{71}\text{Ga}$  nucleus, its isotropic chemical shift ( $\delta_i$ ), and the correlation time ( $\tau_c$ ) of the bound metal ion in each case. In three of the four cases, we also showed that one can obtain  $^{69}\text{Ga}$   $\chi$  values from detectable (though extremely broad) ovotransferrin-bound  $^{69}\text{Ga}$  peaks and their corresponding  $^{71}\text{Ga}$  signals at one field ( $B_0 = 11.7$  T). Moreover, the  $^{71}\text{Ga}$   $\chi$  data for protein-bound  $\text{Ga}^{3+}$  and a model complex,  $\text{Ga}(\text{acac})_3$ , were used to compute the electric field gradient ( $eq_{\text{ionic}}$ ) at the bound metal ion in each case; these values are placed in the context of our earlier  $^{27}\text{Al}$  and  $^{45}\text{Sc}$  NMR studies of ovotransferrin (Aramini, J. M.; Vogel, H. J. *J. Am. Chem. Soc.* **1994**, *116*, 1988–1993).

### Introduction

Transferrins, which comprise serotransferrin (sTf),<sup>1</sup> ovotransferrin (OTf), and lactoferrin (ITf), are a unique family of large (MW  $\approx 80\,000$ ) nonheme iron-binding proteins that play an integral role in both the transport of iron and defense against bacterial infection in animals.<sup>2</sup> These bilobal, monomeric proteins tenaciously ( $K_D \leq 10^{-20}$  M) yet reversibly bind two  $\text{Fe}^{3+}$  ions per molecule, one in each of the homologous lobes. The key trait which distinguishes transferrins from other metalloproteins is the requirement and direct participation of a "synergistic anion" (i.e., carbonate) in metal ion binding. The recent flurry of X-ray crystallographic studies on human ITf<sup>3</sup> and the N-terminal half-molecules of rabbit sTf,<sup>4</sup> chicken OTf,<sup>5</sup> and human ITf<sup>6</sup> have painted a much clearer picture of the

structure (and its relation to function) of these proteins. Within a deep interdomain cleft in both lobes of the transferrin molecule, the metal ion is bound in a ternary complex to the anion (bidentate) and the side chains of four highly conserved residues: one Asp, one His, and two Tyr. The six ligands (five oxygens and one nitrogen) are distributed around the metal ion in a distorted octahedral geometry. A further intriguing property of transferrins is their ability to efficiently chelate a wide range of metal ions in addition to  $\text{Fe}^{3+}$ ; this, of course, has implications regarding their participation in the sequestering of other cations, such as  $\text{Ga}^{3+}$ , *in vivo*.

In the last two decades a number of interesting medicinal properties of gallium compounds have been established, carving a niche for this metal in diagnostic and therapeutic medicine.<sup>7</sup> A radioactive isotope of gallium,  $^{67}\text{Ga}$ , has long been recognized as an effective tracer in the diagnosis of certain cancers, in particular lymphomas, and infections.<sup>8</sup> Recently, the ability of  $^{67}\text{Ga}$  imaging to detect pulmonary *Pneumocystis carinii* pneumonia in immunologically suppressed patients has catalyzed interest in the applicability of this technique to the diagnosis of AIDS and AIDS-related complexes.<sup>9</sup> Furthermore, antitumor activity has been documented for gallium salts, such as  $\text{Ga}(\text{NO}_3)_3$ .<sup>10</sup> This salt is now being used clinically in the treatment of cancer-induced hypercalcemia, a condition not uncommon

\* Author to whom correspondence should be addressed.

<sup>⊗</sup> Abstract published in *Advance ACS Abstracts*, November 1, 1994.

(1) Abbreviations used: NMR, nuclear magnetic resonance; sTf, serotransferrin; OTf, ovotransferrin; ITf, lactoferrin; sTf/2N, N(amino)-terminal half-molecule of serotransferrin; OTf/2N, N(amino)-terminal half-molecule of ovotransferrin; OTf/2C, C(carboxy)-terminal half-molecule of ovotransferrin; AIDS, acquired immunodeficiency syndrome; QCT, quadrupolar central transition; acac, 2,4-pentanedionato; FID, free induction decay; TMS, tetramethylsilane; NTA, nitrilotriacetic acid.

(2) For recent review, see: (a) Baker, E. N.; Lindley, P. F. *J. Inorg. Biochem.* **1992**, *47*, 147–160. (b) De Jong, G.; van Dijk, J. P.; van Eijk, H. G. *Clin. Chim. Acta* **1990**, *190*, 1–46. (c) Harris, D. C.; Aisen, P. In *Physical Bioinorganic Chemistry*; Loehr, T. M., Ed.; VCH Publishers: New York, 1989; Vol. 5, pp 239–351.

(3) Anderson, B. F.; Baker, H. M.; Norris, G. E.; Rice, D. W.; Baker, E. N. *J. Mol. Biol.* **1989**, *209*, 711–734.

(4) Sarra, R.; Garratt, R.; Gorinsky, B.; Jhoti, H.; Lindley, P. *Acta Crystallogr.* **1990**, *B46*, 763–771.

(5) Dewan, J. C.; Mikami, B.; Hirose, M.; Sacchettini, J. C. *Biochemistry* **1993**, *32*, 11963–11968.

(6) Day, C. L.; Anderson, B. F.; Tweedie, J. W.; Baker, E. N. *J. Mol. Biol.* **1993**, *232*, 1084–1100.

(7) Abrams, M. J.; Murrer, B. A. *Science* **1993**, *261*, 725–730.

(8) (a) Scott, A. M.; Larson, S. M. *Radiol. Clin. North Am.* **1993**, *31*, 859–879. (b) Mettler, F. A.; Guiberteau, M. J. *Essentials of Nuclear Medicine Imaging*, 3rd ed.; W. B. Saunders: Philadelphia, PA, 1991; pp 253–267.

(9) Woolfenden, J. M.; Carrasquillo, J. A.; Larson, S. M.; Simmons, J. T.; Masur, H.; Smith, P. D.; Shelhamer, J. H.; Ognibene, F. P. *Radiology* **1987**, *162*, 383–387.

(10) Foster, B. J.; Clagett-Carr, K.; Hoth, D.; Leyland-Jones, B. *Cancer Treat. Rep.* **1986**, *70*, 1311–1319.

to cancer patients in the latter stages of the disease that is marked by dangerously high levels of  $\text{Ca}^{2+}$  in the blood caused by increased bone resorption.<sup>11</sup> Although the mechanism of gallium accumulation in tumors and lesions plus its anti-hypercalcemic activity are unclear,<sup>12</sup> it is widely believed that sTf, the primary shuttle for  $\text{Ga}^{3+}$  (and similar cations, such as  $\text{Al}^{3+}$ ) *in vivo*,<sup>13</sup> and ITf are intimately involved in the physiological response to the presence of this element. This has spurred a number of spectroscopic (UV,  $^{13}\text{C}$  and  $^1\text{H}$  NMR) investigations of the interaction of this metal ion with transferrins over the last decade.<sup>14–18</sup> In addition, the almost identical six-coordinate ionic radii of  $\text{Ga}^{3+}$  and  $\text{Fe}^{3+}$  (0.62 and 0.65 Å, respectively)<sup>19</sup> and, consequently, the extremely high affinity exhibited by human sTf and ITf for  $\text{Ga}^{3+}$  ( $K_D \approx 10^{-20}$ – $10^{-22}$  M),<sup>14,15</sup> make it an ideal diamagnetic (i.e., NMR) probe for the metal ion binding sites of transferrins.

In the last two years, we have shown that the metal ions  $\text{Al}^{3+}$  and  $\text{Sc}^{3+}$  bound to the large transferrins can be directly detected by quadrupolar (i.e.,  $^{27}\text{Al}$  and  $^{45}\text{Sc}$ ) central transition (QCT) NMR spectroscopy, and that physical information regarding the nature of their binding sites in these metalloproteins may be obtained.<sup>20–24</sup> Here we apply this methodology to the two NMR active quadrupolar ( $I = 3/2$ ) nuclei of gallium ( $^{69}\text{Ga}$  and  $^{71}\text{Ga}$ ), in combination with  $^{13}\text{C}$  NMR, to gain insight into the binding of  $\text{Ga}^{3+}$  to ovotransferrin in the presence of two synergistic anions, carbonate and oxalate. Although  $^{69}\text{Ga}$  is more abundant than  $^{71}\text{Ga}$  (60.1 vs 39.9%),<sup>25</sup> the latter exhibits a higher resonance frequency ( $\nu_0$ ) and smaller quadrupole moment ( $Q = 0.106$  vs  $0.168$  b),<sup>25</sup> and thus is the more favorable isotope for NMR.<sup>26</sup> To date,  $^{71}\text{Ga}$  and  $^{69}\text{Ga}$  reports in the literature have been restricted to studies of relatively small complexes in solution and, more recently, solids.<sup>27</sup>

## Experimental Section

**Materials.** Chicken apo-OTf was purchased from Sigma Chemical Co. and used without further purification. OTf/2N and OTf/2C were purified from the tryptic digest of OTf and assigned as previously described.<sup>20,28,29</sup> Tris(2,4-pentanedionato)gallium ( $\text{Ga}(\text{acac})_3$ ) and the

- (11) Todd, P. A.; Fitton, A. *Drugs* **1991**, *42*, 261–273.
- (12) (a) Tsan, M.-F. *J. Nucl. Med.* **1985**, *26*, 88–92. (b) Tsan, M.-F.; Scheffel, U. *J. Nucl. Med.* **1986**, *27*, 1215–1219.
- (13) Jackson, G. E. *Polyhedron* **1990**, *9*, 163–170.
- (14) Harris, W. R.; Pecoraro, V. L. *Biochemistry* **1983**, *22*, 292–299.
- (15) Harris, W. R. *Biochemistry* **1986**, *25*, 803–808.
- (16) Bertini, I.; Luchinat, C.; Messori, L.; Scozzafava, A.; Pellacani, G.; Sola, M. *Inorg. Chem.* **1986**, *25*, 1782–1786.
- (17) Woodworth, R. C.; Butcher, N. D.; Brown, S. A.; Brown-Mason, A. *Biochemistry* **1987**, *26*, 3115–3120.
- (18) Kubal, G.; Mason, A. B.; Patel, S. U.; Sadler, P. J.; Woodworth, R. C. *Biochemistry* **1993**, *32*, 3387–3395.
- (19) Shannon, R. D. *Acta Crystallogr.* **1976**, *A32*, 751–767.
- (20) Aramini, J. M.; Vogel, H. J. *J. Am. Chem. Soc.* **1993**, *115*, 245–252.
- (21) Aramini, J. M.; Vogel, H. J. *Bull. Magn. Reson.* **1993**, *15*, 84–88.
- (22) Aramini, J. M.; Germann, M. W.; Vogel, H. J. *J. Am. Chem. Soc.* **1993**, *115*, 9750–9753.
- (23) Aramini, J. M.; Vogel, H. J. *J. Am. Chem. Soc.* **1994**, *116*, 1988–1993.
- (24) Germann, M. W.; Aramini, J. M.; Vogel, H. J. *J. Am. Chem. Soc.* **1994**, *116*, 6971–6972.
- (25) Mills, I.; Cvtas, T.; Homann, K.; Kallay, N.; Kuchistu, K. *Quantities, Units and Symbols in Physical Chemistry*, 2nd ed.; Blackwell Scientific Pub.: Oxford, 1993; pp 98–104.
- (26) Brevard, C.; Granger, P. *Handbook of High Resolution Multinuclear NMR*; J. Wiley and Sons: New York, 1981.
- (27) For recent reviews, see: (a) Bradley, S. M.; Howe, R. F.; Kydd, R. A. *Magn. Reson. Chem.* **1993**, *31*, 883–886. (b) Akitt, J. W. In *Multinuclear NMR*; Mason, J., Ed.; Plenum Press: New York, 1987; pp 259–292.
- (28) Oe, H.; Doi, E.; Hirose, M. *J. Biochem. (Tokyo)* **1988**, *103*, 1066–1072.
- (29) Thornton, D. J.; Holmes, D. F.; Sheehan, J. K.; Carlstedt, I. *Anal. Biochem.* **1989**, *182*, 160–164.

hydrate of gallic nitrate were purchased from Aldrich Chemical Co. Stock solutions ( $\approx 150$  mM) of gallic chloride were prepared by treating gallium metal (Alfa Inorganics) with concentrated HCl, heating to dryness, and dissolving the white powder in the appropriate volume of doubly distilled water. The suppliers of the  $^{13}\text{C}$ - and  $^2\text{H}$ -labeled compounds and solvents used here are given in our earlier reports.<sup>20,22</sup>

**NMR Spectroscopy.** The concentration of each protein NMR sample ( $\approx 0.3$ – $1.4$  mM in 2.0 mL of 25% v/v  $\text{D}_2\text{O}$ ) was determined spectrophotometrically ( $A_{280}$ ) using extinction coefficients listed elsewhere.<sup>20,28</sup>  $^{13}\text{C}$ ,  $^{69}\text{Ga}$ , and  $^{71}\text{Ga}$  NMR spectra of the proteins were acquired locked and at 25 °C on Bruker AM 400 and AMX 500 NMR spectrometers, each equipped with a 10 mm broadband probe using the following parameters: (1)  $^{13}\text{C}$  ( $\nu_0 = 125.7$  MHz,  $B_0 = 11.7$  T), a 50° flip angle, a repetition time of 2.1 s, a sweep width of 25 kHz, and 16K data points; data was processed with a 7 Hz line broadening; (2)  $^{71}\text{Ga}$  ( $\nu_0 = 122.0$  MHz,  $B_0 = 9.4$  T;  $\nu_0 = 152.5$  MHz,  $B_0 = 11.7$  T) and  $^{69}\text{Ga}$  ( $\nu_0 = 120.0$  MHz,  $B_0 = 11.7$  T), a 45° flip angle, a repetition time of 15 ms, a sweep width of 100 kHz, a 10–15  $\mu\text{s}$  dead time, and 2K data points; in all spectra the carrier frequency was placed either on-resonance or between signals to ensure maximum excitation.  $^{71}\text{Ga}$  and  $^{69}\text{Ga}$  FIDs were zero-filled once and processed with exponential line broadenings of 250 and 500 Hz, respectively. Note that in order to detect the extremely broad protein-bound  $^{71,69}\text{Ga}$  signals (line widths on the order of several kilohertz) we used quite short dead times to prevent appreciable attenuation of the signals. However, under such conditions severe base-line distortions arising from electronic and acoustic ringing<sup>30</sup> appear in spectra obtained using single-pulse experiments, seriously hampering the elucidation of the positions and line widths of the desired signals. Hence, to eliminate this phenomenon we resorted to a novel composite pulse sequence, consisting of three 45° pulses and a 64-step phase cycle.<sup>31</sup> We found that this sequence is superior to previous approaches<sup>32</sup> in terms of its efficacy when pulse lengths shorter than 90° are employed, although one must sacrifice some signal intensity (i.e., in  $^{71}\text{Ga}$  NMR spectra (at either field) of 1 mM  $\text{Ga}^{3+}$ , pH 1.5,  $\approx 50\%$  of the signal is lost when using the composite pulse sequence compared to a one-pulse experiment (45° pulses in both cases); this loss is only 10% if 90° pulses are used). The chemical shifts and line widths of all  $^{71}\text{Ga}$  and  $^{69}\text{Ga}$  NMR signals were obtained by fitting a minimum of four transformations of each data set using the LINESIM routine (written for DISNMR by P. Barron, Bruker Australia), and in some cases with the "ldcon" program (in the Bruker UXNMR software package).  $^{13}\text{C}\{^1\text{H}\}$  (100.6 MHz),  $^{71}\text{Ga}$  (122.0 MHz), and  $^{69}\text{Ga}$  (96.0 MHz) NMR spectra of  $\text{Ga}(\text{acac})_3$  (0.2 M in  $\text{C}_6\text{D}_6$ ) were obtained at 25 °C on the Bruker AM 400 spectrometer.  $^{13}\text{C}$  longitudinal relaxation times ( $T_1$ ) for this complex were determined by the inversion recovery method. All  $^{71}\text{Ga}$  and  $^{69}\text{Ga}$  NMR spectra are referenced to external 1.0 M  $\text{Ga}(\text{NO}_3)_3$  in  $\text{D}_2\text{O}$ ;  $^{13}\text{C}$  chemical shifts are reported with respect to external TMS.

## Theory

The theory and equations pertaining to the relaxation of quadrupolar nuclei with particular emphasis on quadrupolar metal ions bound to large proteins has been described in detail in our earlier reports.<sup>22,23</sup> Briefly, for a half-integer quadrupolar nucleus (nuclear spin,  $I$ , greater than  $1/2$ ) in the far from extreme narrowing limit (when the product of its Larmor frequency,  $\omega_0$ , and its correlation time,  $\tau_c$ , is much larger than unity) that has isotropic motion, relaxation is described by  $I + 1/2$  nondegenerate exponentials, of which that due to the central ( $m = 1/2 \rightarrow -1/2$ ) transition can give rise to an observable signal.<sup>33–35</sup> This signal possesses two extremely important and unique traits. First,

- (30) Gerthofanis, I. P. *Prog. Nucl. Magn. Reson. Spectrosc.* **1987**, *19*, 267–329.
- (31) Zhang, W.; Furó, I. *Biopolymers* **1993**, *33*, 1709–1714.
- (32) Zhang, S.; Wu, X.; Mehring, M. *Chem. Phys. Lett.* **1990**, *173*, 481–484.
- (33) Hubbard, P. S. *J. Chem. Phys.* **1970**, *53*, 985–987.
- (34) Bull, T. E.; Forsén, S.; Turner, D. L. *J. Chem. Phys.* **1979**, *70*, 3106–3111.
- (35) Forsén, S.; Lindman, B. In *Methods of Biochemical Analysis*; Glick, D., Ed.; J. Wiley and Sons: New York, 1981; Vol. 27, pp 289–486.

its line width is inversely proportional to  $\tau_c$  and the square of the nuclear resonance frequency,  $\nu_0$ , and, thus, the external magnetic field,  $B_0$ ; for  $I = 3/2$  nuclei such as  $^{69}\text{Ga}$  and  $^{71}\text{Ga}$  this dependence is<sup>33,35</sup>

$$\Delta\nu_{1/2} = (2.0 \times 10^{-2}) \left( \frac{\chi^2}{\nu_0^2 \tau_c} \right) \quad (1)$$

where  $\chi$  is the quadrupole coupling constant (*vide infra*). Second, the chemical shift of the signal due to the central transition when  $\omega_0\tau_c \gg 1$  is shifted to lower frequency in a field dependent manner. This effect, termed the "second-order dynamic frequency shift" (in parts per million), is given by the following expression ( $I = 3/2$ ):<sup>36,37</sup>

$$\delta_{\text{obs}} - \delta_i = (-2.5 \times 10^4) \left( \frac{\chi^2}{\nu_0^2} \right) \quad (2)$$

where  $\delta_{\text{obs}}$  and  $\delta_i$  are the observed and isotropic (i.e., in the absence of second-order effects) chemical shifts, respectively. Hence, eqs 1 and 2 indicate that an increase in  $B_0$  translates into a decrease in line width and a downfield shift in the signal arising from the central transition. This statement is in fact true for any half-integer quadrupolar nucleus; expressions analogous to eqs 1 and 2 differing only in the magnitudes of the leading coefficients have been derived for higher spin nuclei (i.e.,  $I = 5/2$  and  $7/2$ ).<sup>22,23,38</sup>

In the above relations, the quadrupole coupling constant,  $\chi$ , which is indicative of the symmetry of the electronic environment of the nucleus due to the coordinated ligands, is a product of the electric quadrupole moment of the nucleus,  $eQ$ , and the electric field gradient at the nucleus,  $eq_{\text{obs}}$ ; the latter in turn can be expressed as a function of the actual electric field gradient due to the local ionic charges,  $eq_{\text{ionic}}$ , and a factor, the Sternheimer antishielding factor  $1 - \gamma_\infty$ , that accounts for the distortion from spherical symmetry of the inner electron orbitals induced by the valence electrons (eq 3).<sup>39</sup>

$$\chi = \frac{e^2 Q q_{\text{obs}}}{h} = \frac{e^2 Q q_{\text{ionic}} (1 - \gamma_\infty)}{h} \quad (3)$$

By inspection of eqs 1–3, it is apparent that both the resonance position ( $\delta_{\text{obs}}$ ) and detectability ( $\Delta\nu_{1/2}$ ) of a quadrupolar nucleus in the limit of slow isotropic motion are dependent on a number of crucial intrinsic nuclear ( $I$ ,  $Q$ ,  $\nu_0$ ), atomic ( $1 - \gamma_\infty$ ) and molecular ( $eq_{\text{ionic}}$ ,  $\tau_c$ ) properties, and on a key experimental variable ( $\nu_0$  via  $B_0$ ).

## Results

**$\text{Ga}^{3+}$  and Carbonate Binding to OTf, Followed by  $^{13}\text{C}$  and  $^{71}\text{Ga}$  NMR at 11.7 T.** When a sample of apo-OTf that contains  $^{13}\text{C}$ -enriched carbonate is titrated with aqueous  $\text{GaCl}_3$ , one observes two signals in the carbonyl region of the  $^{13}\text{C}$  NMR spectrum ( $\delta = 166.07$  and  $165.91$  ppm), as well as a pair of broad overlapping  $^{71}\text{Ga}$  signals ( $\delta = -103$  and  $-128$  ppm; Figure 1). These resonances correspond to  $^{13}\text{CO}_3^{2-}$  and  $\text{Ga}^{3+}$ , respectively, bound in slow exchange to the two sites of the protein. Both probes reveal that under these conditions metal ion binding proceeds in a sequential manner. Note that in the

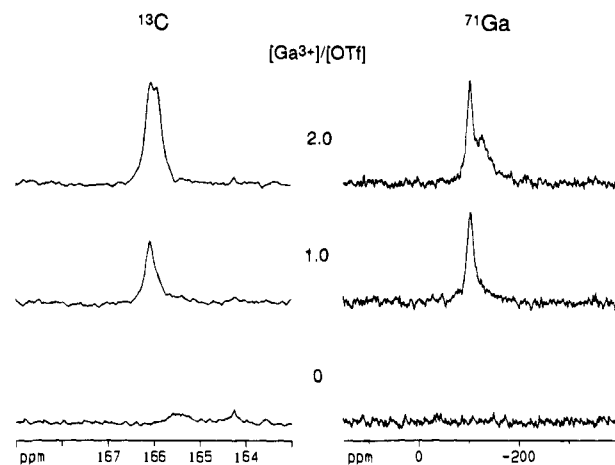


**Figure 1.** Titration of apo-OTf (1.28 mM, 20 mM  $\text{Na}_2^{13}\text{CO}_3$ , pH 7.6) with  $\text{Ga}^{3+}$  monitored by  $^{13}\text{C}$  (125.7 MHz; 10 000 scans each) and  $^{71}\text{Ga}$  (152.5 MHz; 1 500 000 scans each) NMR. Only an expansion of the carbonyl region is shown in each  $^{13}\text{C}$  NMR spectrum.

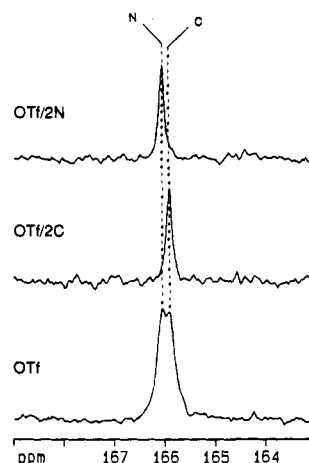


**Figure 2.** Expanded carbonyl regions of the  $^{13}\text{C}$  (125.7 MHz) NMR spectra of OTf (1.28 mM, 2.0 equiv of  $\text{Ga}^{3+}$ , 20 mM  $\text{Na}_2^{13}\text{CO}_3$ , pH 7.6, 10 000 scans), OTf/2C (0.35 mM, 1.0 equiv of  $\text{Ga}^{3+}$ , 2 mM  $\text{Na}_2^{13}\text{CO}_3$ , pH 7.8, 30 000 scans), and OTf/2N (0.35 mM, 1.0 equiv of  $\text{Ga}^{3+}$ , 10 mM  $\text{Na}_2^{13}\text{CO}_3$ , pH 7.7, 28 000 scans).

presence of excess  $\text{Ga}^{3+}$ , an additional  $^{71}\text{Ga}$  signal at  $\delta = 223$  ppm is observed at pHs above 7.5, corresponding to  $\text{Ga}(\text{OH})_4^-$  (spectra not shown). Using our standard half-molecule approach,<sup>20,21,23,40</sup> we have assigned the high- and low-frequency  $^{13}\text{C}$  signals to the bound anion in the N- and C-terminal sites of the protein, respectively (Figure 2). Thus, in the presence of carbonate the N-lobe of OTf binds  $\text{Ga}^{3+}$  with higher affinity than the C-lobe. Because of this site preference, the  $^{13}\text{C}$  NMR experiments on OTf/2N and OTf/2C also indirectly afford an assignment of the  $^{71}\text{Ga}$  signals in Figure 1. The  $^{13}\text{C}$  and  $^{71}\text{Ga}$  NMR data for the  $\text{Ga}^{3+}$ /carbonate form of OTf are listed in Table 1.

**Experiments with Oxalate as the Synergistic Anion.**  $^{13}\text{C}$  and  $^{71}\text{Ga}$  NMR spectroscopy were also used to examine the  $\text{Ga}^{3+}$ /oxalate forms of OTf, OTf/2C, and OTf/2N. For the intact protein one observes two pairs of closely spaced doublets in the carbonyl region of the  $^{13}\text{C}$  NMR spectrum, each of which lines up perfectly with signals from the same derivative of one of the half-molecules of OTf (spectra not shown; see Table 1). This pattern of resonances corresponds to the two (nonequivalent) carbonyl carbons of this anion bound in a 1,2-bidentate

(36) Werbelow, L. G. *J. Chem. Phys.* **1979**, *70*, 5381–5383.

(37) Werbelow, L. G.; Pouzard, G. *J. Phys. Chem.* **1981**, *85*, 3887–3891.

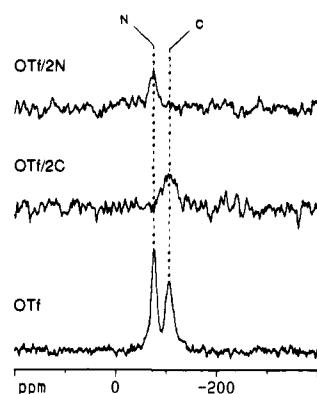
(38) Westlund, P.-O.; Wennerström, H. *J. Magn. Reson.* **1982**, *50*, 451–466.

(39) Lucken, E. A. C. *Nuclear Quadrupole Coupling Constants*; Academic Press: New York, 1969; pp 79–96.

(40) Aramini, J. M.; Krygsman, P. H.; Vogel, H. J. *Biochemistry* **1994**, *33*, 3304–3311.

**Table 1.**  $^{13}\text{C}$  and  $^{71}\text{Ga}$  NMR Data for the  $\text{Ga}^{3+}/^{13}\text{CO}_3^{2-}$  and  $\text{Ga}^{3+}/^{13}\text{C}_2\text{O}_4^{2-}$  Derivatives of OTf at 11.7 T

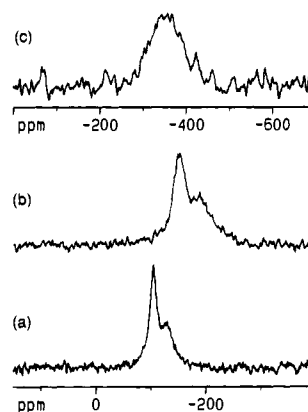
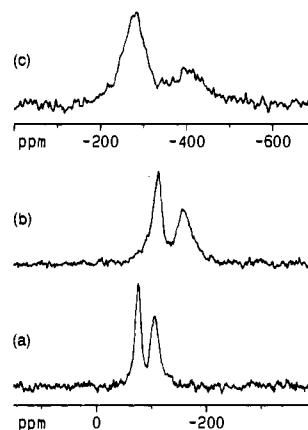
protein	anion	site	$\delta(^{13}\text{C})$ (ppm)	$^1J_{\text{C-C}}$ (Hz)	$\delta(^{71}\text{Ga})$ (ppm)	$\Delta\nu_{1/2}$ (Hz)
OTf	$^{13}\text{CO}_3^{2-}$	N	166.07		-103	1900
		C	165.91		-128	4200
OTf	$^{13}\text{C}_2\text{O}_4^{2-}$	N	167.90	73	-76	1400
			165.69	73		
		C	167.74	73	-107	2300
			165.10	73		
OTf/2N	$^{13}\text{CO}_3^{2-}$		166.07		nd <sup>a</sup>	nd
		$^{13}\text{C}_2\text{O}_4^{2-}$	167.90	73	-76	2500
OTf/2C	$^{13}\text{CO}_3^{2-}$		165.91		nd	nd
		$^{13}\text{C}_2\text{O}_4^{2-}$	167.74	73	-106	5000
			165.10	73		

<sup>a</sup> Not determined.**Figure 3.**  $^{71}\text{Ga}$  (152.5 MHz) NMR spectra of OTf (1.30 mM, 2.0 equiv of  $\text{Ga}^{3+}$ , 10 mM  $\text{Na}_2^{13}\text{C}_2\text{O}_4$ , pH 7.6, 1 500 000 scans), OTf/2C and OTf/2N (0.35 mM, 1.0 equiv of  $\text{Ga}^{3+}$ , 2.5 mM  $\text{Na}_2^{13}\text{C}_2\text{O}_4$ , pH 7.6–7.7, 2 500 000 scans each).

fashion to the metal ion in both sites of the protein.<sup>40–42</sup> In the  $^{71}\text{Ga}$  NMR spectrum ( $B_0 = 11.7$  T) of the intact protein one again observes two broad, well-resolved signals ( $\delta = -76$  and  $-113$  ppm), which can be assigned to the N- and C-lobes of OTf from analysis of the half-molecules (Figure 3). Note that the bound  $^{71}\text{Ga}$  signals for OTf/2N and OTf/2C are appreciably broader than the resonances due to the corresponding sites in the intact protein (Table 1). In contrast to the titration results with carbonate presented above, we found that both sites of OTf bind  $\text{Ga}^{3+}$  with comparable affinity in the presence of oxalate (data not shown).

#### $^{71}\text{Ga}$ and $^{69}\text{Ga}$ NMR of OTf at Two Magnetic Fields.

$^{71}\text{Ga}$  ( $B_0 = 11.7$  T) and  $^{69}\text{Ga}$  ( $B_0 = 11.7$  T) NMR spectra of the  $\text{Ga}^{3+}$ /carbonate and  $\text{Ga}^{3+}$ /oxalate forms of OTf are shown in Figures 4 and 5. For each protein-bound  $^{71}\text{Ga}$  signal, a decrease in magnetic field results in a substantial upfield shift and increase in line width, in agreement with the predicted behavior of a half-integer quadrupolar nucleus under far from extreme narrowing conditions (*vide supra*). With the chemical shifts ( $\delta_{\text{obs}}$ ) and line widths ( $\Delta\nu_{1/2}$ ) of these signals at two fields in hand, we have calculated values of  $\delta_i$ ,  $\chi$  (eq 2), and  $\tau_c$  (eq 1) for the metal ion bound to both sites of OTf and in the presence of either anion; these data are listed in Table 2. The known quadrupole moments ( $Q$ ) of  $^{71}\text{Ga}$  and  $^{69}\text{Ga}$  allow us to easily compute values of  $\chi$  for the latter isotope, and from the isotropic chemical shift of each resonance, we can employ eq 2 to obtain an estimate of where the corresponding  $^{69}\text{Ga}$  signal for each

**Figure 4.**  $^{71}\text{Ga}$  and  $^{69}\text{Ga}$  NMR spectra of the  $\text{Ga}^{3+}$ /carbonate form of OTf (1.34 mM, pH 7.8) at two magnetic fields: (a)  $^{71}\text{Ga}$ ,  $B_0 = 11.7$  T, 1 500 000 scans; (b)  $^{71}\text{Ga}$ ,  $B_0 = 9.4$  T, 5 000 000 scans; (c)  $^{69}\text{Ga}$ ,  $B_0 = 11.7$  T, 4 000 000 scans.**Figure 5.**  $^{71}\text{Ga}$  and  $^{69}\text{Ga}$  NMR spectra of the  $\text{Ga}^{3+}$ /oxalate form of OTf (1.30 mM, pH 7.6) at two magnetic fields: (a)  $^{71}\text{Ga}$ ,  $B_0 = 11.7$  T, 1 500 000 scans; (b)  $^{71}\text{Ga}$ ,  $B_0 = 9.4$  T, 5 000 000 scans; (c)  $^{69}\text{Ga}$ ,  $B_0 = 11.7$  T, 4 000 000 scans.

species will resonate (Table 2). Indeed, we find excellent agreement between the calculated and empirical values of the OTf-bound  $^{69}\text{Ga}$  signals. Notice that in each case the line width of the  $^{69}\text{Ga}$  resonance is significantly larger than the  $^{71}\text{Ga}$  signal for the same adduct as expected from eq 1; in fact, the  $^{69}\text{Ga}$  signal for the metal ion bound to the C-site of the protein with carbonate as the synergistic anion is broadened beyond detectability. From the observed  $^{71}\text{Ga}$  and  $^{69}\text{Ga}$  chemical shifts of the three signals on the higher field instrument one can again use eq 2 to deduce  $\chi$  for  $^{69}\text{Ga}$  (Table 2).

**Effect of Pulse Length on OTf-Bound  $^{71}\text{Ga}$  Signals.** The choice of pulse length is an important consideration in this work, since we<sup>20,23</sup> and others<sup>43</sup> have previously shown that the intensities of signals due to transferrin-bound quadrupolar nuclei ( $^{27}\text{Al}$ ,  $^{45}\text{Sc}$ , and  $^{51}\text{V}$ ) reach a maximum at pulse lengths far shorter than  $90^\circ$  when a single excitation pulse is used. Indeed, for  $^{71}\text{Ga}$  NMR spectra of  $(\text{Ga}^{3+})_2\text{-OTf-(}^{13}\text{CO}_3^{2-})_2$  acquired at a field of 9.4 T with the composite pulse sequence using different flip angles, we found virtually no signal when using  $90^\circ$  flip angles, in contrast to the spectra in this report acquired with  $45^\circ$  pulses. Moreover, under identical conditions ( $45^\circ$  composite pulses), the combined area of the  $^{71}\text{Ga}$  signals for the  $\text{Ga}^{3+}$ /carbonate adduct of OTf is only 29% that of a sample of  $\text{Ga}(\text{NO}_3)_3$  that contains an equimolar amount of  $\text{Ga}^{3+}$  (data not shown); this value is comparable to the theoretically predicted intensity (40%) due to the  $m = 1/2 \rightarrow -1/2$  transition of a  $I = 3/2$  nucleus.<sup>35,36</sup>

(41) Dubach, J.; Gaffney, B. J.; More, K.; Eaton, G. R.; Eaton, S. S. *Biophys. J.* **1991**, *59*, 1091–1100.(42) Shongwe, M. S.; Smith, C. A.; Ainscough, E. W.; Baker, H. M.; Brodie, A. M.; Baker, E. N. *Biochemistry* **1992**, *31*, 4451–4458.(43) Butler, A.; Eckert, H. *J. Am. Chem. Soc.* **1989**, *111*, 2802–2809.

**Table 2.**  $^{71}\text{Ga}$  and  $^{69}\text{Ga}$  NMR Data for the  $\text{Ga}^{3+}$ /Carbonate and Oxalate Derivatives of Ovotransferrin<sup>a</sup>

site	anion	$^{71}\text{Ga}$ NMR <sup>b</sup> ( $B_0 = 9.4$ T)		$\delta_i$ (ppm)	$\chi(^{71}\text{Ga})$ (MHz)	$\tau_c$ (ns)	$\chi_{\text{calc}}(^{69}\text{Ga})$ (MHz)	$\delta_{\text{calc}}(^{69}\text{Ga})$ ( $B_0 = 11.7$ T) (ppm)	$^{69}\text{Ga}$ NMR ( $B_0 = 11.7$ T)		$\chi(^{69}\text{Ga})$ (MHz)
		$\delta_{\text{obs}}$ (ppm)	$\Delta\nu_{1/2}$						$\delta_{\text{obs}}$ (ppm)	$\Delta\nu_{1/2}$ (Hz)	
N	$^{13}\text{CO}_3^{2-}$	-151	2800	-19	8.8	39	14.0	-359	-354	9500	13.9
C	$^{13}\text{CO}_3^{2-}$	-192	6000	-14	10.3	29	16.3	-475	n.o. <sup>c</sup>	n.o.	nd <sup>d</sup>
N	$^{13}\text{C}_2\text{O}_4^{2-}$	-113	2000	-10	7.8	49	12.4	-277	-279	6500	12.5
C	$^{13}\text{C}_2\text{O}_4^{2-}$	-162	3400	-9	9.5	40	15.1	-405	-398	12000	14.9

<sup>a</sup> For the values of  $\chi$ ,  $\delta_i$ , and  $\tau_c$  due to  $\text{Ga}^{3+}$  bound to the N-lobe of OTf with carbonate as the synergistic anion,  $\delta$  (-57 ppm) and  $\Delta\nu_{1/2}$  (860 Hz) data for this signal at 17.6 T were included in the calculations (see ref 24). <sup>b</sup>  $^{71}\text{Ga}$  NMR data for these adducts at 11.7 T are listed in Table 1. <sup>c</sup> Not observed. <sup>d</sup> Not determined.

**Table 3.** Electric Field Gradients for  $\text{Ga}(\text{acac})_3$  and the  $\text{Ga}^{3+}/^{13}\text{CO}_3^{2-}$  and  $\text{Ga}^{3+}/^{13}\text{C}_2\text{O}_4^{2-}$  Forms of OTf

complex	anion	$\chi(^{71}\text{Ga})$ (MHz)	$ eq_{\text{obs}} $ ( $10^{20}$ V/m <sup>2</sup> ) <sup>a</sup>	$ eq_{\text{ionic}} $ ( $10^{20}$ V/m <sup>2</sup> ) <sup>b</sup>
$\text{Ga}(\text{acac})_3$		6.5	25.4	2.1
$\text{Ga}^{3+}$ -OTf N	$^{13}\text{CO}_3^{2-}$	8.8	34.3	2.8
$\text{Ga}^{3+}$ -OTf C	$^{13}\text{CO}_3^{2-}$	10.3	40.2	3.3
$\text{Ga}^{3+}$ -OTf N	$^{13}\text{C}_2\text{O}_4^{2-}$	7.8	30.4	2.5
$\text{Ga}^{3+}$ -OTf C	$^{13}\text{C}_2\text{O}_4^{2-}$	9.5	37.1	3.0

<sup>a</sup> Calculated using a quadrupole moment,  $Q$ , for  $^{71}\text{Ga}$  of 0.106 b (ref 25). <sup>b</sup> Calculated using a Sternheimer factor,  $1 - \gamma_{\infty}$ , for  $\text{Ga}^{3+}$  of 12.3 (ref 47).

**Experiments with  $\text{Ga}(\text{acac})_3$ .** We have obtained  $^{69}\text{Ga}$  and  $^{71}\text{Ga}$   $\chi$  values for a model octahedral  $\text{Ga}^{3+}$  complex,  $\text{Ga}(\text{acac})_3$ ,<sup>44</sup> by  $^{13}\text{C}$ ,  $^{69}\text{Ga}$ , and  $^{71}\text{Ga}$  NMR spectroscopy. Using the correlation time of this molecule ( $\tau_c = 43$  ps), deduced from the  $T_1$  relaxation time of the  $^{13}\text{C}$  signal due to the methine carbons ( $\delta = 100.22$  ppm),<sup>45</sup> we calculated the quadrupole coupling constants for both gallium isotopes from the line widths of the  $^{69}\text{Ga}$  and  $^{71}\text{Ga}$  peaks for the bound metal ion in this complex ( $\delta(^{69}\text{Ga}) = -14$  ppm,  $\Delta\nu_{1/2}(^{69}\text{Ga}) = 5400$  Hz,  $\chi(^{69}\text{Ga}) = 10.0$  MHz;  $\delta(^{71}\text{Ga}) = -13$  ppm,  $\Delta\nu_{1/2}(^{71}\text{Ga}) = 2250$  Hz,  $\chi(^{71}\text{Ga}) = 6.5$  MHz).<sup>45</sup> Our results are quite comparable to data reported some time ago for  $\text{Ga}(\text{acac})_3$ .<sup>46</sup> Table 3 lists the values of  $eq_{\text{obs}}$  and  $eq_{\text{ionic}}$  for  $^{71}\text{Ga}$  in  $\text{Ga}(\text{acac})_3$  and the N- and C-sites of OTf in the presence of either carbonate or oxalate computed with eq 3 from the  $^{71}\text{Ga}$   $\chi$  data for each, the quadrupole moment of this nucleus, and the Sternheimer antishielding factor for  $\text{Ga}^{3+}$  ( $1 - \gamma_{\infty} = 12.3$ ).<sup>47</sup>

## Discussion

In this report, we have for the first time demonstrated the feasibility of directly detecting  $\text{Ga}^{3+}$  bound to a large metalloprotein through the central transitions of its NMR active

(44) Dymock, K.; Palenik, G. J. *Acta Crystallogr.* **1974**, *B30*, 1364-1366.

(45) The correlation time of the  $\text{Ga}(\text{acac})_3$  can be calculated from the  $^{13}\text{C}$   $T_1$  for the methine carbons, which relax solely by heteronuclear dipole-dipole relaxation, using the following equation:

$$\frac{1}{T_1^{\text{DD}}} = \left( \frac{\mu_0}{4\pi} \right)^2 \left( \frac{N_{\text{H}} \gamma_{\text{H}}^2 \gamma_{\text{C}}^2 \hbar^2 \tau_c}{r_{\text{CH}}^6} \right)$$

where the C-H bond distance ( $r_{\text{CH}}$ ) is assumed to be 1.09 Å (Levy, G. C.; Lichter, R. L.; Nelson, G. L. *Carbon-13 Nuclear Magnetic Resonance Spectroscopy*, 2nd ed.; J. Wiley and Sons: New York, 1980; pp 211-246). This may then be used to obtain the  $^{71}\text{Ga}$  quadrupole coupling constants using the expression for the relaxation of a quadrupolar nucleus under extreme narrowing conditions ( $\omega_0 \tau_c \ll 1$ ):

$$\Delta\nu_{1/2} = \frac{3\pi}{10} \frac{(2I+3)}{I^2(2I-1)} \chi^2 \tau_c$$

(See: Abragam, A. *Principles of Nuclear Magnetism*; Oxford University Press: Oxford, U.K., 1961; pp 313-315; ref 35 herein).

(46) Dechter, J. J.; Henrickson, U.; Kowalewski, J.; Nilsson, A.-C. *J. Magn. Reson.* **1982**, *48*, 503-511.

(47) Schmidt, P. C.; Sen, K. D.; Das, T. P.; Weiss, A. *Phys. Rev. B* **1980**, *22*, 4167-4179.

isotopes. We have also shown that in this special case there is a second route, aside from the field dependence of the observed chemical shifts, for extracting physical information ( $\chi$  and  $\delta_i$ ) regarding the protein-bound quadrupolar metal nucleus, namely, from the difference in  $\delta_{\text{obs}}$  for the bound  $^{71}\text{Ga}$  and  $^{69}\text{Ga}$  signals at one (preferably high) magnetic field. Recently, an analogous solid-state version of this approach has been successfully applied to the study of gallosilicates.<sup>48,49</sup> The very broad  $^{71}\text{Ga}$  signals reported here illustrate a potential pitfall in working with  $I = 3/2$  nuclei, which, in general, are hampered by larger line widths and second-order dynamic frequency shifts compared to higher spin nuclei. Even with the benefit of special pulse sequences, our work suggests that resonances limited to line widths of  $\leq 10$  kHz can be adequately detected with the instrumentation used. Certainly, such difficulties can well be circumvented by resorting to higher field spectrometers.<sup>24</sup>

The multinuclear NMR techniques used highlight a number of interesting facets of the interactions of transferrins with tripositive metal cations, such as  $\text{Ga}^{3+}$ . First, as we noted earlier,<sup>20</sup> the enhanced resolution offered by high-field instruments is best suited for discriminating between the near-degenerate  $^{13}\text{C}$  signals in the  $\text{M}^{3+}/^{13}\text{CO}_3^{2-}$  form of transferrins, as opposed to earlier attempts.<sup>16</sup> Second, similar to the published  $\text{Al}^{3+}$  binding properties of OTf and human sTf,<sup>20,50,51</sup> the N-site of OTf binds  $\text{Ga}^{3+}$  much more proficiently than the C-site when carbonate serves as the synergistic anion. We find that this site preference is abolished when the titration is conducted with oxalate in the sample, in contrast to our results for  $\text{Al}^{3+}$ ,<sup>20</sup> and a recent  $^1\text{H}$  NMR study which reported the preferential binding of  $\text{Ga}^{3+}$  (administered as the NTA complex) to the C-site of human sTf.<sup>18</sup> However, caution must be exercised when interpreting such data in light of the numerous studies concerning the selectivity of metal ion binding in transferrins, and how for the same metal ion (i.e.,  $\text{Fe}^{3+}$ ) this may be altered by the nature of the donor complex (as well as pH, ionic strength, and indeed, the type of transferrin).<sup>2c</sup> Third, the isotropic chemical shifts of the OTf-bound  $^{71}\text{Ga}$  NMR signals fall well within the range diagnostic of  $\text{Ga}^{3+}$  bound to six oxygen-containing ligands ( $\delta \approx 40$  to  $-80$  ppm),<sup>27a</sup> as one would expect based on the documented structural features of the metal ion binding sites in transferrins.<sup>3-6</sup> In addition, the small dispersion in the values of  $\delta_i$  suggests that differences in the observed resonance positions for either protein-bound gallium isotope are largely due to second-order effects (i.e., differences in  $\chi$ ).<sup>22,23</sup> Next, the empirical correlation times for  $\text{Ga}^{3+}$  bound to OTf ( $\tau_c \approx 30$ -50 ns) are in good agreement with previous studies.<sup>22,23,52</sup> Finally, from the  $^{71}\text{Ga}$  (and  $^{69}\text{Ga}$ )  $\chi$  and  $eq_{\text{ionic}}$  data one can construct the following trend for the

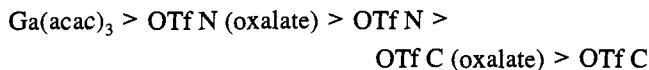
(48) Timken, H. K. C.; Oldfield, E. *J. Am. Chem. Soc.* **1987**, *109*, 7669-7673.

(49) Kentgens, A. P. M.; Bayense, C. R.; van Hooff, J. H. C.; de Haan, J. W.; van de Ven, L. J. M. *Chem. Phys. Lett.* **1991**, *176*, 399-403.

(50) Ichimura, K.; Kihara, H.; Yamamura, T.; Satake, K. *J. Biochem. (Tokyo)* **1988**, *103*, 50-54.

(51) Kubal, G.; Mason, A. B.; Sadler P. J.; Tucker, A.; Woodworth, R. C. *Biochem. J.* **1992**, *285*, 711-714.

symmetries of the  $\text{Ga}^{3+}$  binding sites in the compounds analyzed (in order of decreasing symmetry):



However, the quadrupole coupling constants reported here (see Table 2) are appreciably larger than those for tetrahedral  $\text{Ga}^{3+}$  in gallium analog zeolites ( $\chi(^{71}\text{Ga}) = 1.2\text{--}2.2$  MHz;  $\chi(^{69}\text{Ga}) = 1.9\text{--}3.5$  MHz).<sup>48,49</sup> Unlike our earlier results for  $\text{Al}^{3+}$  ( $r = 0.54$  Å)<sup>19</sup> and  $\text{Sc}^{3+}$  ( $r = 0.75$  Å)<sup>19</sup> binding to OTf,<sup>20,22,23</sup> the above series suggests that in either site the ligand environment of the  $\text{Ga}^{3+}$  is more symmetric when oxalate is the anion compared to carbonate. Nevertheless, the resulting electric field

(52) Schwab, F. J.; Appel, H.; Neu, M.; Thies, W.-G. *Eur. Biophys. J.* **1992**, *21*, 147–154. Our results are also in good agreement with  $\tau_c$  values for a variety of proteins recently determined by  $^{13}\text{C}$  NMR (Wang, S. X.; Stevens, A.; Schleich, T. *Biopolymers* **1993**, *33*, 1581–1589).

gradients are very comparable to  $^{27}\text{Al}$  data for OTf ( $eq_{\text{ionic}} = 2.7\text{--}3.7 \times 10^{20}$  V/m<sup>2</sup>); these values are, however, much larger than the field gradients for the larger  $\text{Sc}^{3+}$  ion bound to OTf ( $eq_{\text{ionic}} = 1.4\text{--}1.8 \times 10^{20}$  V/m<sup>2</sup>).<sup>22</sup> Moreover, for both  $\text{Al}^{3+}$  and  $\text{Ga}^{3+}$ , the acac complex possesses the lowest value of  $eq_{\text{ionic}}$ , suggesting that the central metal ion is situated in a more symmetric (octahedral) environment compared to the protein-bound metal ion, in contrast to  $\text{Sc}^{3+}$ .

**Acknowledgment.** This research was supported by the Medical Research Council of Canada (MRC). The AM 400 and AMX 500 NMR spectrometers used in this work were purchased with funds provided by the MRC and the Alberta Heritage Foundation for Medical Research (AHFMR). J.M.A. is the recipient of a studentship from the AHFMR. H.J.V. is an AHFMR scholar. We thank Ms. Jillian A. Saponja for her assistance in purifying the OTf/2N and OTf/2C samples used in this study.